

Supplemental Information

Direct examination of the relevance for folding, binding and electron transfer of a conserved protein folding intermediate

Emilio Lamazares^{1,2}, Sonia Vega¹, Patricia Ferreira^{1,2}, Milagros Medina^{1,2}, Juan J. Galano^{1,2}, Marta Martínez-Júlvez^{1,2}, Adrián Velázquez-Campoy^{1,2,3,4} & Javier Sancho^{1,2,4*}

¹Biocomputation and Complex Systems Physics Institute (BIFI)-Joint Units: BIFI-IQFR (CSIC) and GBsC-CSIC, Universidad de Zaragoza, Zaragoza, Spain

²Departamento de Bioquímica y Biología Molecular y Celular, Facultad de Ciencias, Universidad de Zaragoza, Zaragoza, Spain

³Fundación ARAID, Gobierno de Aragón, Spain

⁴Aragon Health Research Institute (IIS Aragón), Universidad de Zaragoza, Zaragoza, Spain

Table S1: Thermal unfolding of WT and 6M apo and holoflavodoxins^a

Protein ^a	DSC three-state fit					DSC two-state fit		
	[FMN] (μ M)	ΔH_{NI} (kcal/mol)	T_{mNI} ($^{\circ}$ C)	ΔH_{IU} (kcal/mol)	T_{mIU} ($^{\circ}$ C)	ΔH_{ND} (kcal/mol)	T_{mND} ($^{\circ}$ C)	$\Delta H_{vH}/\Delta H_{cal}$ ^b
WT	-	27.8 \pm 0.3	47.9 \pm 1.3	59.1 \pm 0.5	56.0 \pm 0.8	-	-	-
	40	-	-	-	-	101.9 \pm 0.6	67.5 \pm 0.08	1.09
	80	-	-	-	-	104.3 \pm 0.3	67.9 \pm 0.02	1.17
	120	-	-	-	-	106.6 \pm 0.3	68.3 \pm 0.02	1.17
6M	-	-	-	-	-	87.6 \pm 0.1	70.3 \pm 0.10	1.06 (1.02) ^c
	40	-	-	-	-	124.4 \pm 0.2	73.2 \pm 0.02	1.07 (1.08) ^c
	80	-	-	-	-	128.3 \pm 0.2	73.8 \pm 0.01	1.21 (1.22) ^c
	120	-	-	-	-	129.2 \pm 0.2	74.3 \pm 0.02	1.31 (1.28) ^c

^a Protein concentration: 40 μ M

^b van't Hoff enthalpies, ΔH_{vH} , determined as in Table 2 from ref. ¹. Calorimetric enthalpies, ΔH_{cal} , determined from the thermograms in Fig. 4.

^c Unlike commonly assumed, the ratio of van't Hoff and calorimetric enthalpies of a two-state protein that binds a ligand non-covalently (e.g. apoflavodoxin binding FMN) is not always of 1.0 but it increases with the concentration of free ligand (not shown). The actual value of the ratio for a two-state protein can be calculated at a given ligand concentration if both the binding and stability parameters are known. For 6M flavodoxin, the ratios calculated assuming a two-state unfolding equilibrium coupled to ligand binding are those in parenthesis, which closely correspond to the experimentally determined ones.

Table S2. Midpoint reduction potentials of WT and 6M flavodoxins

Variant	$E_{\text{ox/sq}}$ (mV)	$E_{\text{sq/hq}}$ (mV)
WT	-275±5	-452±5
6M	-325±5	-413±5

Table S3. Interaction data of complexes
between wild type FNR and flavodoxin variants

Variant	K_b (M^{-1})	ΔH (kcal/mol)
WT	$2.0(\pm 0.4) \times 10^5$	5.0 ± 0.6
6M	$1.9(\pm 0.4) \times 10^5$	2.1 ± 0.6

Table S4. Data collection and refinement statistics for
6M holoflavodoxin

Data collection statistics

Space group	P 2 ₁ 2 ₁ 2 ₁
Cell dimensions <i>a</i> , <i>b</i> , <i>c</i> (Å)	37.92 62.91 64.65
Wavelength, Å	0.9791
Resolution, Å	64.65 – 1.1 (1.16 – 1.1)
Total no. of reflections	472026 (66547)
No. of unique reflections	62821 (8885)
Redundancy	7.5 (7.5)
Completeness, %	99.0 (97.4)
Average I/σ	18.1 (4.6)
R _{merge} ^a	0.047 (0.431)
CC (1/2)	0.999 (0.933)

Refinement statistics

Resolution range, Å	45.1-1.1
Protein non-hydrogen atoms	1327
Ligand non-hydrogen atoms	31
Solvent non-hydrogen atoms	123
R _{work} (%)	16.1
R _{free} ^b (%)	17.6
rmsd bond length, Å	0.016
rmsd bond angles, °	1.699
Average B-factor, Å ²	13.93

Values in parentheses correspond to the highest resolution shell.

^a $R_{\text{merge}} = \Sigma (I - I_{\text{av}}) / \Sigma I_{\text{av}}$, where the summation is over symmetry-equivalent reflections

^b R calculated for 5% of data excluded from the refinement.

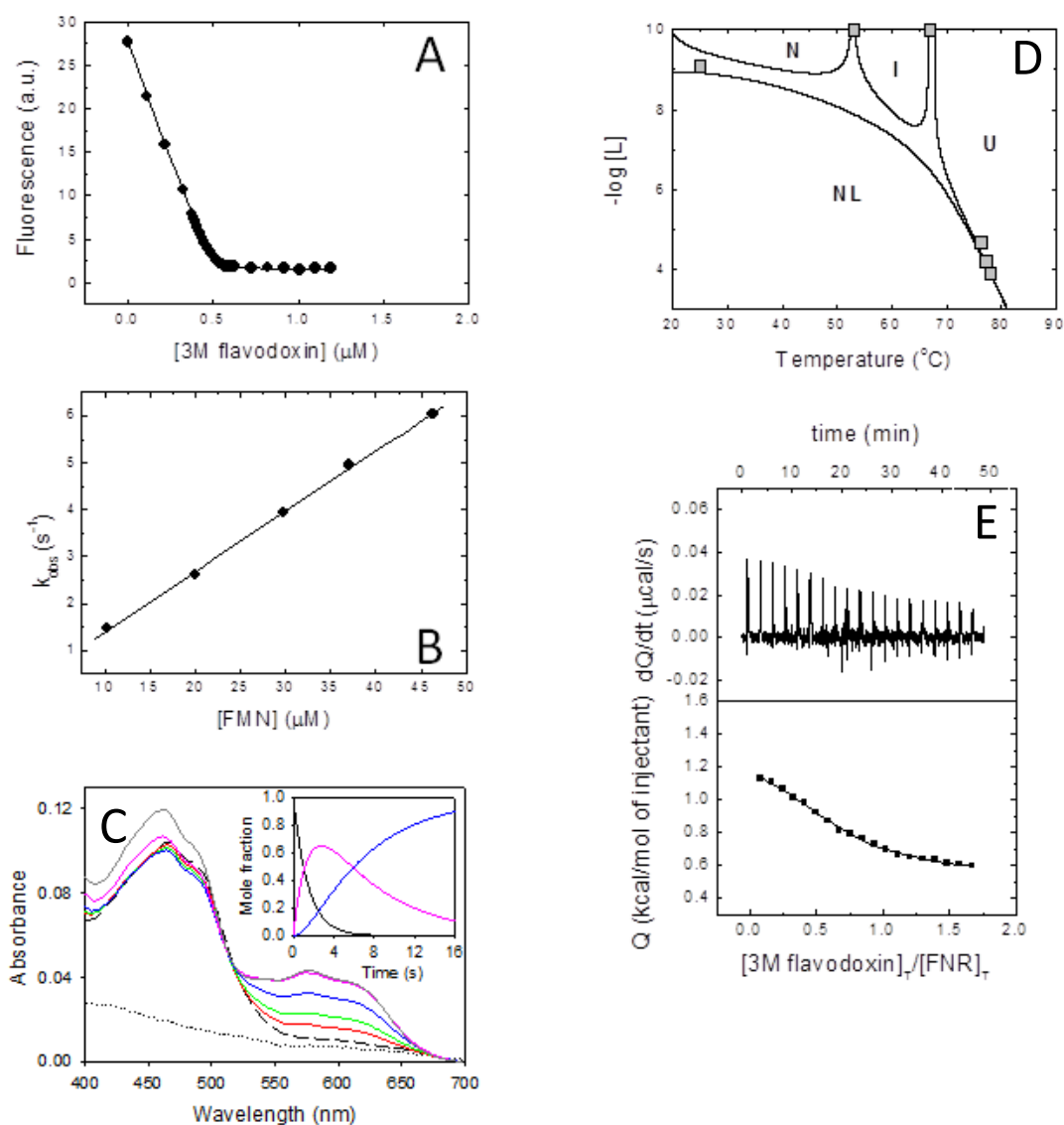


Fig. S1. Properties of the 3M apoflavodoxin variant carrying three (E20K/E72K/D126K) of the six mutations present in 6M flavodoxin. (A) Titration of FMN binding to 3M apoflavodoxin in 50 mM MOPS, pH 7.0, at 25 $^{\circ}\text{C}$, by following the quenching of emission fluorescence at 525 nm. (B) Secondary plot used to calculate k_{on} for FMN binding to 3M apoflavodoxin from a linear fit (solid line) of the observed kinetic binding constants at different concentrations of FMN (filled circles). (C) Spectral time course of the anaerobic reduction of Fld $_{\text{ox}}$ 3M variant by FNR $_{\text{hq}}$. The mixing molar ratio was 1:1 with a final concentration of $\sim 10 \mu\text{M}$ for each protein. The spectrum of FNR $_{\text{hq}}$ before mixing is shown as a black dotted line and the first spectrum after mixing as a black dashed line. Spectra after mixing are shown at 0.015, 0.34, 0.66, 1.55, 5.13 and 16.00 seconds. The inset shows the evolution of the kinetically distinguishable species obtained by global analysis of the reaction to a two steps (A \rightarrow B \rightarrow C) model. A, B and C species are shown in black, pink, and blue lines, respectively. (D) Temperature-ligand concentration phase diagram for 3M flavodoxin showing the coupling between the folding and binding equilibria at pH 8.0. The phase separation lines (or coexistence lines) between the different regions (N, unliganded native: apoflavodoxin; NL, liganded native: holoflavodoxin; I, partly unfolded native basin intermediate; and U, unfolded) represent the conditions (temperature-ligand concentration) where certain species (N, NL, I, or U) reach 50 % of the total population of molecules. (E) Isothermal calorimetric titration of the interaction between FNR and 3M holoflavodoxin. The experiment was performed in 50 mM Tris/HCl, pH 8.0, at 25 $^{\circ}\text{C} \pm 0.1 ^{\circ}\text{C}$ with 20 μM FNR in the calorimetric cell and 200 μM 3M holoflavodoxin in the syringe.

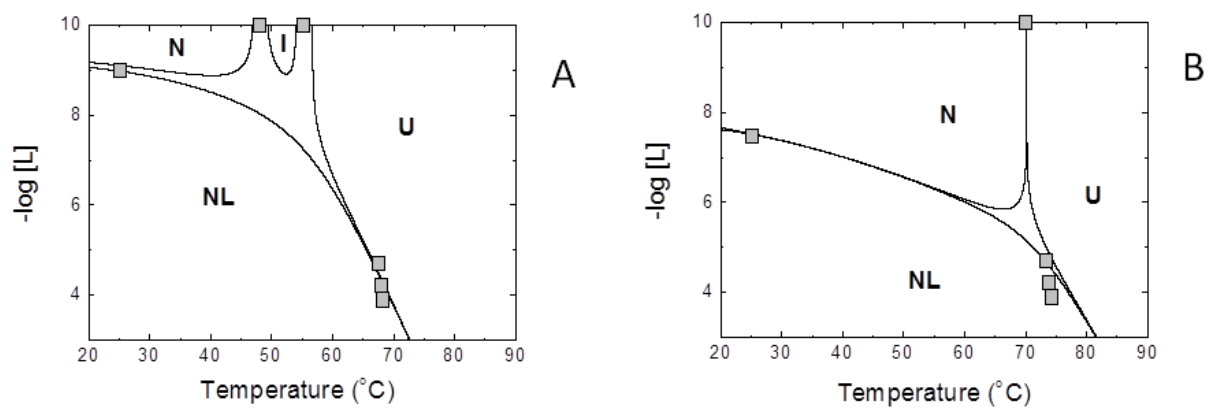


Fig. S2: Temperature-ligand concentration phase diagrams for WT (A), and 6M (B) flavodoxin showing the coupling between the folding and binding equilibria. The phase separation lines between the different regions (N, unliganded native or apoflavodoxin; NL, liganded native or holoflavodoxin; I, native basin partly unfolded intermediate; and U, unfolded) represent the conditions (temperature-ligand concentration) where a given species (N, NL, I, or U) reaches 50 % of the total population of molecules.

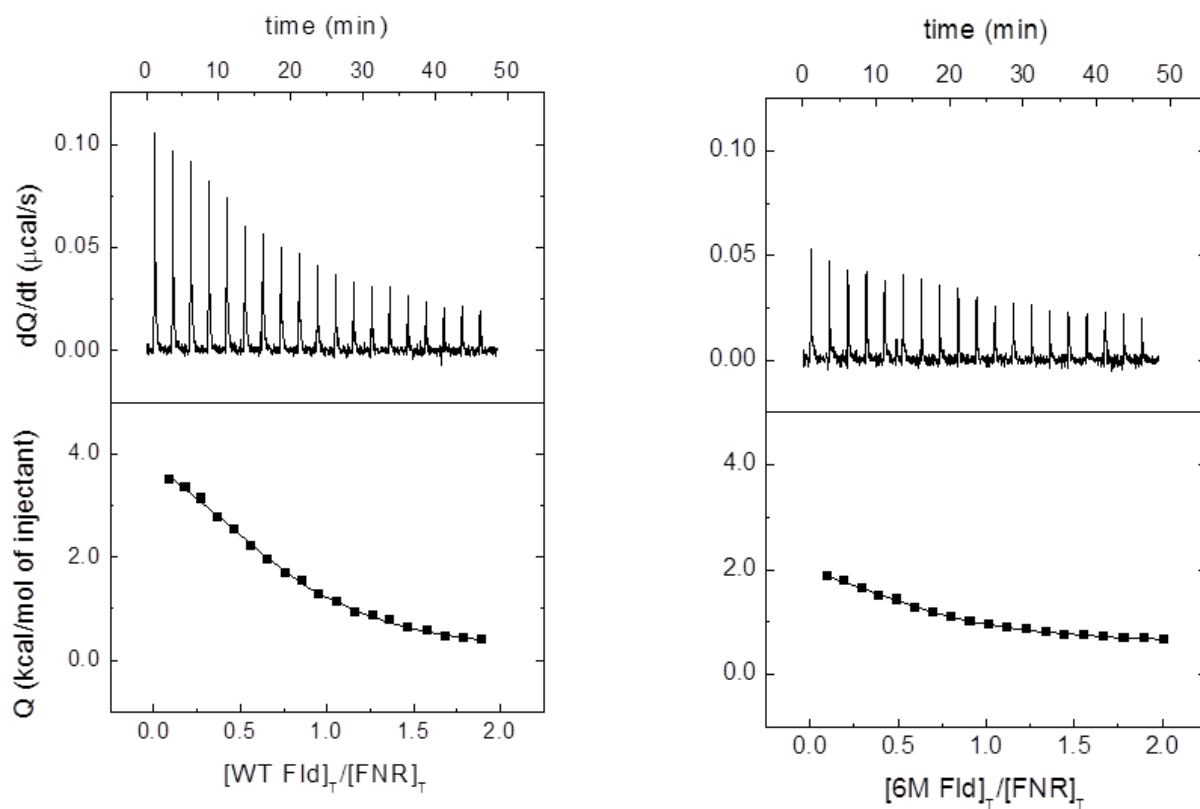


Fig. S3. Isothermal calorimetric titrations of the interaction between FNR and WT (left) or 6M flavodoxin (right). The experiments were performed in 50 mM Tris/HCl, pH 8.0, at $25\text{ }^{\circ}\text{C} \pm 0.1\text{ }^{\circ}\text{C}$ with $20\text{ }\mu\text{M}$ FNR in the calorimetric cell and $200\text{ }\mu\text{M}$ of either WT or 6M holoflavodoxin in the syringe.

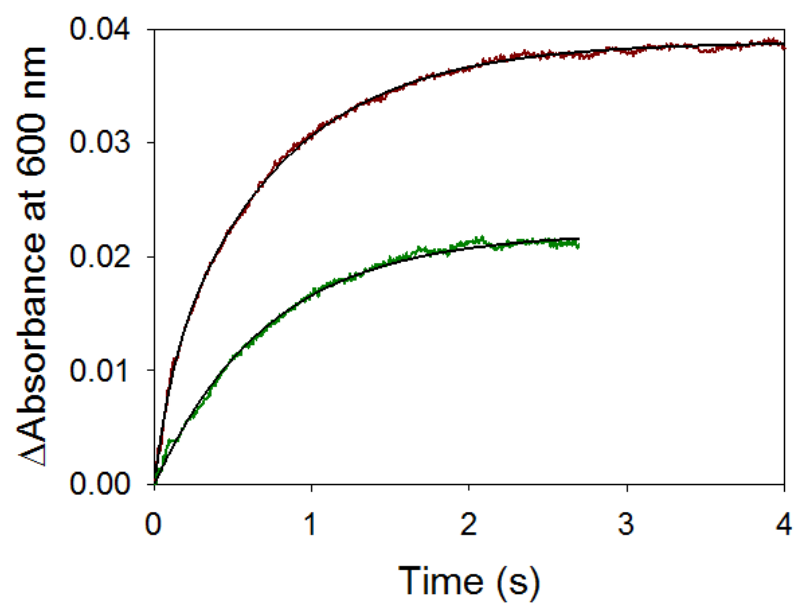


Fig. S4. Time course for the semiquinone formation kinetics between WT Fld_{ox} (dark red line) and its 6M variant (green line) with WT FNR_{hq}. Fits are shown as black lines. The assays were followed in stopped-flow under anaerobic conditions in 50 mM Tris/HCl, pH 8.0, at 12 °C.

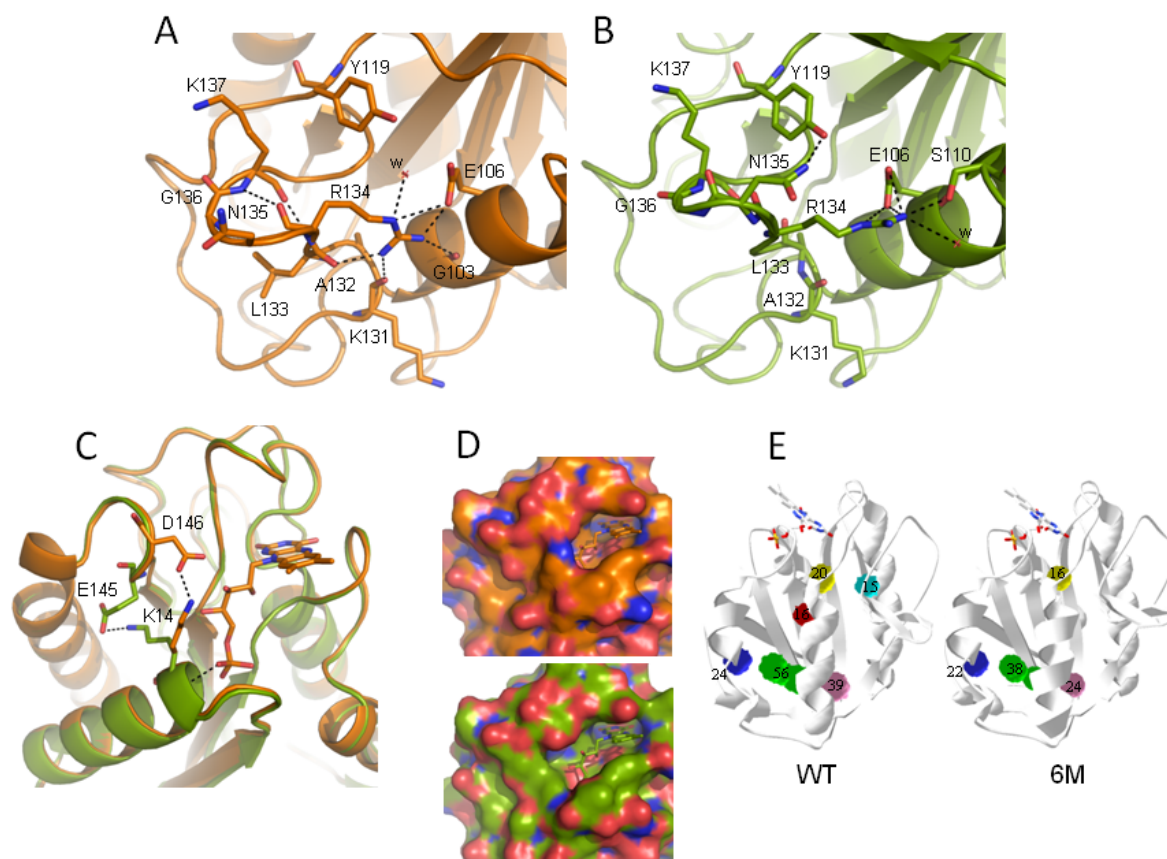


Fig. S5. Cartoon detail of the structures of (A) 6M (orange) and (B) WT (green) flavodoxins. Residues forming loop 133-137 are shown in CPK colored sticks and H-bonds as dashed lines. (C) Network of H-bonds around K14 in the superposition of 6M (orange) and WT (green). The FMN cofactor shown in sticks belongs to the 6M structure. (D) Detail of the molecular surface at the FMN binding site in 6M (orange C atoms) and WT (green C atoms). (E) Distribution of cavities present in WT and 6M structures. Numbers on cavities indicate their corresponding volumes in \AA^3 .

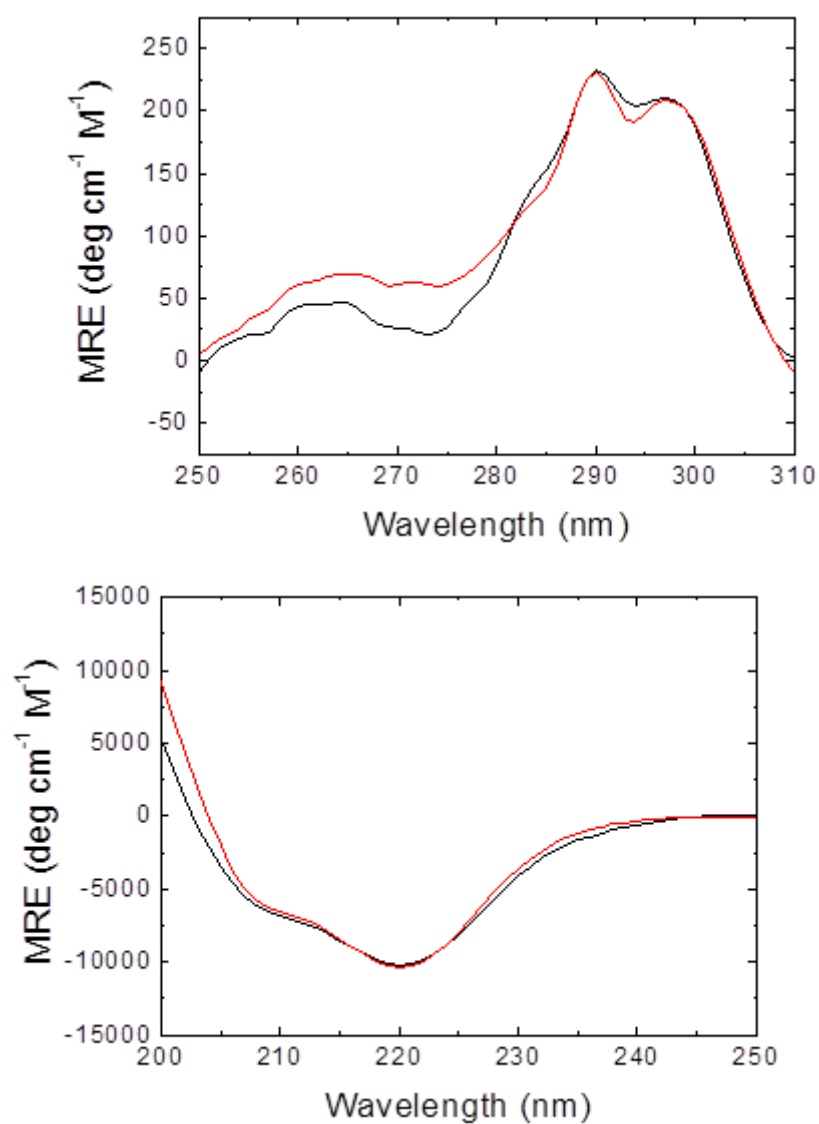


Fig. S6. Circular dichroism spectra of WT (red line) and 6M apoflavodoxin (green line) recorded in 50 mM MOPS pH 7.0 (top, near-UV spectra) and 5 mM MOPS, pH 7.0 with 15 mM NaCl (bottom, far-UV spectra) at 25 °C ± 0.1 °C.